Incorporating Safety Reliability into Route Choice Model: Heterogeneous Crash Risk Aversions

Helai Huang[1], Chunyang Han[1], Guangming Xu[1]*, Mengxi Jiang[2], S.C. Wong[3], Md Mazharul Haque[4]

1. School of Traffic and Transportation Engineering, Smart Transport Key Laboratory of Hunan Province, Central South University, Changsha, 410075, China

2. Chengdu Municipal Engineering and Research Design Institute, Chengdu, China.

3. Department of Civil Engineering, The University of Hong Kong, Pokfulam Road, Hong Kong, China.

4. School of Civil Engineering and Built Environment, Queensland University of Technology, 2 George Street, Brisbane City, QLD, 4001, Australia

* Corresponding Author (Guangming Xu): E-mail: xuguangming@csu.edu.cn

Abstract: In this study, a route choice model which accounts for both travelers' safety concern—route safety reliability—and travel time concern is proposed. Route safety reliability (variability) is defined by the distribution of the travel crash risk cost (CRC) to represent the safety condition of travel routes. We further associate the travel safety variability due to stochastic crash occurrence with travelers' crash risk aversion route choice behaviors, and postulate that travelers acquire the variability of route travel safety based on the past experience and factor it into their route choice in the form of an effective crash risk cost (effective CRC). This effective crash cost is formed depending on travelers' requirements on safe arrivals, and thus varies with individuals and trip specific factors (e.g. purposes). Moreover, all travelers want to minimize the summing of their travel time and their effective CRC. A route-based solution algorithm is designed to solve the route choice model. Two networks including Nguyen and Dupis' network and Sioux falls network are conducted as numerical studies to illustrate the model. The results show that (1) the travelers' route choice behaviors are sensitive to the route safety performance, including the average safety condition (the mean of the CRC distribution) and safety reliability (the standard deviation of the CRC distribution); (2) the safety performance of movements at intersection would significantly influence the travelers' route choice decisions; and (3) travelers with different safety attitudes (heterogeneous crash risk aversions) would make different route choice decisions.

Keyword: traffic assignment method; safety reliability; heterogeneous risk aversion; effective crash risk cost

1. INTRODUCTION

Numerous route choice models have long been developed for traffic assignment on a network according to travel demand. Researchers postulate that travelers tend to choose the most effective route to minimize their travel cost. Different types of cost-effective routes have been studied, such as the least cost travel time (Goczyłla and Cielatkowski, 1995), eco-friendly routes (Tzeng and Chen, 1993; Rilett and Benedek, 1994; Nie and Li, 2013) and the most reliable routes (Lo and Tung, 2003; Shao et al., 2006; Chen and Zhou, 2010). However, few studies have been reported for how safety aspects could be quantified into trip planning of travelers, even though travel safety is undoubtedly an essential for travelers to measure the performance of candidate routes. In other words, conventional route choice models are not suitable for representing traveler's route choice behavior regarding their safety concern. This demand of research becomes more realistic and urgent when accurate and individual-based safety information could be available for pre-trip and en-route phases in the upcoming era of intelligent and connected vehicles (Gerla et al., 2014; Park et al., 2018; Elliott et al., 2019).

Travel safety is considered as 'crash risk potential' of a vehicle navigating through streets and intersections (Chandra, 2014). Crash prediction model has been extensively used to evaluate the safety performance of a site, facility or roadway network by estimating the expected average crash frequency of investigated site type given traffic exposure and associated risk factors (AASHTO, 2014). However, this technique aims to reflect the safety aspect of an objectively underlying road property, similar to capacity, which has a nature of long-term average. Only using the aspect of the safety property of a road site to indicate the crash risk potential that an individual traveler might encounter may be inadequate. Recently, predicting the probability of a crash occurring during a short period is becoming increasingly common in crash risk estimation (Lee et al., 2003; Abdel-Aty and Pemmanaboina, 2006; Payyanadan et al., 2017; Hossain et al., 2019). This method associates the potential of having a crash with several traffic characteristics and their real-time status, reflecting the crash risk via an estimated value. Nevertheless, crashes are rare and random events. Crashes occur as a function of a set of events that are influenced by a large number of factors. These factors are partly deterministic and measurable; but partly stochastic (i.e., data maybe uncollectable or unavailable) (Huang and Abdel-Aty, 2010; Mannering and Bhat, 2014; Han et al., 2018). Moreover, many of these relevant factors, such as traffic, road user behavior, vehicle fleet and weather, change autonomously over time, and some even change on a continual basis. The variation of factors over time would result in uncertainty of crash occurrence. An estimated certain value may be inefficient to represent such uncertainty during a trip. It is difficult to accurately predict how safe a trip is.

In fact, these stochastic or random variations both of measurable factors and those factors that cannot be predicted add variability to crash risk potential. This variation naturally tends to randomly fluctuate around an expected value. This expected value is the embodiment of a usual, normal or average safety condition of road site, and can be materialized by relevant conditions of the properties of the road site. The unpredictable fluctuation is closely linked to the related risk factors and their recurrent variations, which reflects the reliability of safety performance of the road site. In such cases, travelers cannot predict what the exact crash risk potential along a route is; but they may have the knowledge (for the familiar route) of safety reliability of a route based on past experience or informed by the real-time safety status of selectable route. For example, travelers figure out (or be informed) that certain routes contain mixed traffic flows or needs high workloads (e.g. in snowy mountain highway) during driving tend to induce high crash risk and travel safety variability. They may then factor such variability into their route planning and settle into their habitual routing plans for their daily commute. In forming their habitual routing plans, travelers select routes to lower both their mean crash risk potential and travel safety variability.

The reliability of a particular route has been found to play an important role in traveler's choice behavior (Jackson and Jucker, 1982; Abdel-Aty et al., 1997). Route choice models based on reliability assumptions and concepts have received considerable attention over the last two decades, such as the proposed travel time budget (TTB) traffic equilibrium model (Smith et al., 2008; Nie, 2011; Carrion and Levinson, 2012; Lo et al., 2006; Shao et al., 1985; Xu et al., 2018) which defines the reliability aspect of travel time variability in the route choice decision process, and the so-called α-reliable mean-excess model that explicitly considers both reliability and/or unreliability aspects of travel time variability (Chen and Zhou, 2010; Chen et al., 2011; Xu et al., 2014a; Xu et al., 2014b; Xu et al., 2017). However, the efforts have been made only on the concern about travel efficiency—how much time (cost) do travelers spend on route, and traveler's route choice behaviors that aim to increase travel efficiency—how can a trip be finished more quickly. Moreover, in the context of traffic safety research, most studies have only focused on objectively evaluating the safety reliability of road entities (Jovanović, 2011; Oh and Mun, 2012; Bačkalić et al., 2014; Yu et al., 2016; Jalayer and Zhou, 2016). When individual's travel safety becomes a primary concern for the traveler—how much probability a trip can be finished safely, understanding how traveler's safety-concern behavior in coping with travel safety reliability affects the performance of the overall transportation system would be extremely essential for transport planners and transport system managers. To fill this research gap, this paper provides a basis by formulating and solving a route choice model which incorporates such safety-consideration route choice behavior.

In this study, we develop a route choice model which accounts for both travelers' travel safety concern—route safety reliability—and travel time concern. In particular, route safety reliability (variability) is defined by the distribution of the travel crash risk cost (CRC) to represent the safety condition of travel routes. The mean of the distribution represents the expected average safety condition of a road network element, while the standard deviation reflects its safety reliability. These two parameters are determined according to the classical safety evaluation approach. Specifically, the parameters of the CRC distribution of segments are quantified by using the proposed average-speed-based crash risk model, and those of turning links are defined by accounting for the risk effect of the traffic volume. Furthermore, the mean-and-variance-based effective CRC is applied to model travelers' evaluation of different routes for different crash risk aversions. The effective CRC relates to the traveler's crash risk aversion which depends on the characteristics of travelers and the trip features (e.g. trip purpose). It was assumed that all travelers want to minimize their effective CRC and travel time in the choice of routes. Correspondingly, an algorithm has been designed and tested for solving the proposed route choice model. In the end, we explore the effect on the overall network performance by including this safety consideration in the modeling of route choice.

The rest of this paper is organized as follows. Section 2 develops the formulation. Section 3 proposes the solution method of developed formulation. Numerical experiments are given in Section 4. Finally, Section 5 contains concluding remarks.

2. FORMULATION

2.1. Travel safety quantification

2.1.1 Notation

The notations used throughout the paper are listed as follows, unless otherwise specified.

G	road network
V	set of nodes
A	set of links
$a \rightarrow b$	turning and crossing movements at a node
W	set of origin-destination (OD) pairs
p_w	set of all single routes between O-D pair w
$\bar{A}$	set of turning and crossing movements
v_a	average speed of vehicles on link a
r_a	CRC of link a
t_a	travel time of link a with flow q_a
$r_{a\rightarrow b}$	CRC of an intersection turning movement $a \rightarrow b$
$E(r_a)$	mean CRC per exposure unit of link a
σ_a	standard deviation of CRC per exposure unit of link a
$E(x_{a\rightarrow b})$	mean CRC of an intersection turning movement $a \rightarrow b$
$\sigma_{a\rightarrow b}$	standard deviation of CRC of an intersection turning movement $a \rightarrow b$
$\gamma/\bar{\gamma}$ and $\tau/\bar{\tau}$	adjustment coefficient
$\eta_a/\bar{\eta}_a$	parameters of traveler's risk perceptions
$\omega_{a\rightarrow b}/\bar{\omega}_{a\rightarrow b}$	parameters of traveler's safety reliability perceptions
r_p	CRC of route p
δ_a^p	route-link incidence parameter
$\delta_{a\rightarrow b}^p$	route-turn incidence parameter
$E(r_p)$	mean CRC of route p

σ_p	standard deviation of CRC of route p
R_p	effective CRC of route p
λ	degree of risk aversion of travelers
ρ	probability that the actual trip CRC is within the specified CRC R_p
S_p	standard normal variate of r_p
R_p^m	effective CRC of m class travelers of route p
λ^m	degree of risk aversion of m class travelers
C_p^m	generalized travel cost of m class travelers of route p
T_p	travel time of route p
θ	cost converting factor of travel time
t_a^0	free-flow travel time of link a
c_a	capacity of link a
α and β	deterministic parameters in BPR function
f_p^m	traffic flow on route p
μ_w^m	minimum generalized cost of class m travelers of all the routes linking O-D pair w
q_w^m	O-D demand
x_a	flows of link a
$x_{a\to b}$	flows of intersection turning movement $a \to b$ at intersections

2.1.2 Road network representation

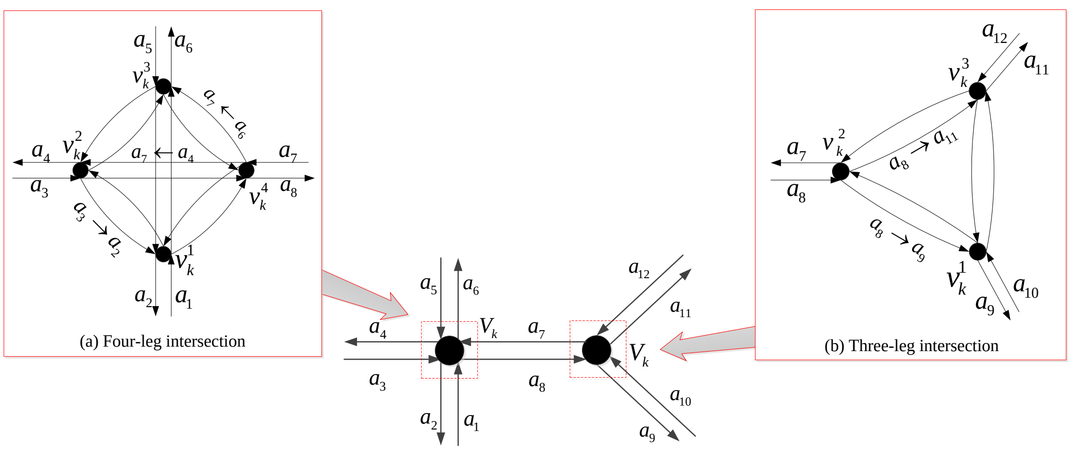

Fig. 1 Model description about link and node turn

A road network consists of a number of individual intersections and road segments, referred to as 'sites'. Assume a road network represented by a directed graph $G = (V, A)$, as shown in Fig. 1, where V and A, respectively, denote the set of nodes and links which can be regarded respectively as intersections and road segments. Fig. 1 also shows the micro representation of the intersections, where each turning or crossing movement at a node can be represented by a dummy link of two connected segments a and b, i.e. $a \to b$. For example, for the four-leg intersection in Fig. 1(a), there are three movement classes including left-turn, right-turn and crossing movement. For link a_1, the left-turn movement is represented by a dummy link $a_1 \to a_4$. Denote $\bar{A}$ as the set of turning and crossing movements at the intersections. Then a route p can be represented as $\{a_1, a_1 \to a_2, a_2, a_2 \to a_3, a_3, \dots, a_i \to a_{i+1}, \dots, a_{n-1}, a_{n-1} \to a_n, a_n\}$ which consist of the set of links $\{a_1, a_2, \dots, a_{n-1}, a_n\}$ and the dummy links $\{a_1 \to a_2, a_2 \to a_3, \dots, a_i \to a_{i+1}, \dots, a_{n-1} \to a_n\}$. For the road network $G = (V, A)$, let W denotes the set of origin-destination (O-D) pairs and p^w denotes the set of all single route between O-D pair w, $w \in W$.

2.1.3 Link and route crash risk distribution

(1) Safety evaluation model

For a transportation system, the safety is defined as the product of the probability of having a crash per unit of exposure (crash risk) and the number of units of exposure occurring on the system during the specified period of time (Chapman, 1973; Hauer, 1982; Hauer, 2002):

$$\text{Safety of system} = \text{Crash risk of system} \times \text{Number of exposure units of system.} \tag{1}$$

For travelers, the crash risk is determined by factors related to their characteristics (e.g. gender, age or driver experience), driving conditions (e.g. travel speed) and road features (or environmental factors, such as weather). The exposure factors measure the likelihood of the traveler being involved in a dangerous or hazardous situation, thus a reliable and meaningful comparison of safety risk between different travelers (Chipman et al., 1992; Qin et al., 2004; Hong et al., 2016). Traffic volume (Qin et al., 2004; Wong et al., 2007) and travel time (Chipman et al., 1992; Xin et al., 2012) are usually used as proxies for exposure.

(2) Crash risk cost distribution

As set forth in the introduction, this study aims to model the flow pattern of travelers who acquire information on the route travel safety, factor this into their route choice consideration, and settle into a long-term habitual equilibrium pattern. The link flows and route flows are associated with this long-term habitual equilibrium flow pattern. Therefore, the link and route safety should be properly represented from the view of travelers.

In the aforementioned transportation network modeled by a directed graph $G = (V, A)$, due to the intrinsic features such as predesigned geometry and specified traffic flow pattern, each link, $a \in A$ or $a \to b \in \bar{A}$, has a certain average crash risk under a specific driving condition. This average safety condition can be estimated according to the features of the road and is related to the traveler's driving conditions (e. g. travel speed). However, for each traveler on the link, the crash risk is random, because the stochastic factors introduce variability into the safety. The individual safety condition of a traveler is difficult to accurately evaluate or predict (Huang and Abdel-Aty, 2010; Mannering and Bhat, 2014; Han et al., 2018). When planning a trip, travelers may not only consider the average crash risk of each link, but also its variability. They may have knowledge based on experience about the safety reliability (variability) of a link and factor such variability into their travel plan.

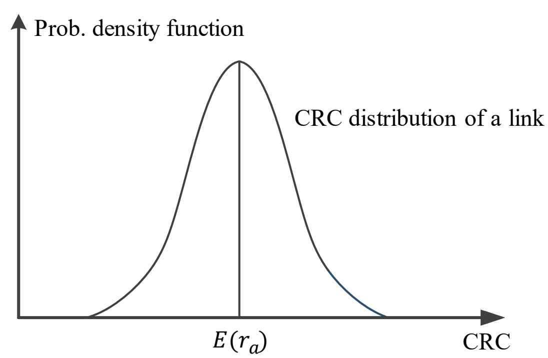

Fig. 2 CRC distribution with mean CRC $E(r_a)$

According to the discussion above, we use the social costs (e.g., the incurred monetary losses and time spent) of crash occurrence to indicate the level of crash risk, referred to as the crash risk cost (CRC). The CRC gives a more psychologically realistic assessment of traveler's decision-making, rather than only using the crash frequency or severity. In this study, we assume the CRC to follow a distribution with a mean value and variance, denoted the CRC distribution:

$$r \sim Dist(E(r),\ \sigma^2) \tag{2}$$

where r is the CRC, $E(r)$ is the mean CRC, which is related to the safety aspects of the road properties and the traveler's local travel situation, and σ^2 is the variance of the CRC, which represents the safety reliability. Fig. 2 presents the example of a normal distribution with its mean value and deviation. Such a CRC distribution can properly describe the average safety condition and safety reliability and thus is closely in accord with travelers' subjective perception of travel crash risk.

(3) CRC distribution of road segment

Following the definition of Eq. (2), we first introduce the CRC distribution for the road segment which is expressed as:

$$r_a \sim Dist_1(E(r_a),\ \sigma_a{}^2)\ \ \forall a \in A \tag{3}$$

where r_a denotes the CRC of road segment a. $E(r_a)$ is the expected mean CRC of segment a; and σ_a is the standard deviation of the CRC of segment a. In this study, the safety evaluation model (Eq.1) is used as the framework to quantify the mean and variance of the CRC distribution. Specifically, travel time is used as the exposure variable, because the time exposure can explain the crash risk variance among drivers with different driving patterns and environments (Chipman et al., 1992; Xin et al., 2012). The travel time of segment a is calculated by using the Bureau of Public Roads (BPR) link performance function:

$$t_a = t_a^0\left[1 + \alpha\left(\frac{x_a}{c_a}\right)^{\beta}\right] \tag{4}$$

where t_a is the travel time of segment a with flow x_a; t_a^0 is the free-flow travel time, which is deterministic; c_a is the capacity of link a; α and β are deterministic parameters.

In regard to the mean CRC per unit of exposure, travel speed has not only been found in many empirical studies to be associated with the crash occurrence, it is also one of the most important factors, in travelers' minds, that influence the travel safety (Aljahani et al., 1999; Elvik, 2002; Charlton and Starkey, 2016; Xu et al., 2019). Based on the actual risk function built via a meta-analysis conducted by Elvik et al. (2004), we proposed an average-speed-based crash risk model to quantify the relationship between the segment average speed and travelers' perception of the mean CRC:

$$\text{Mean CRC/Unit of exposure} = \gamma v_a{}^{\eta_a} \tag{5}$$

where v_a is the average travel speed of vehicles on segment a, which is obtained by dividing the travel time t_a by the segment length l_a. γ is the adjustment coefficient, and η_a is a parameter determined by travelers' risk perception of driving on segment a with speed v_a according to their long-term experience (and is assumed to take a value higher than 1). Fig. 3 shows the perception curve output by Eq. (5), which is evidently plausible. Two conditions are met: 1) the perceived mean CRC grows with the average speed and; 2) the perceived mean CRC grows faster when the average speed is already high. This model supports the use of the CRC distribution to better depict travelers' perceived crash risk.

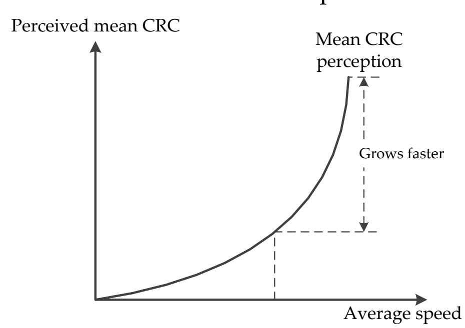

Fig. 3 Relationship between mean CRC and average speed for a road segment

Correspondingly, the mean CRC of segment link a is expressed as:

$$E(r_a) = t_a \gamma v_a{}^{\eta_a} \tag{6}$$

Unfortunately, few empirical studies have investigated the safety reliability in regard to travelers' perceptions. We assume that the perceived CRC variance per unit of exposure is also associated with the segment average speed, which is expressed as:

$$\text{CRC variance} / \text{Unit of exposure} = \bar{\gamma} {v_a}^{\bar{\eta}_a} \tag{7}$$

where $\bar{\gamma}$ is the adjustment coefficient; $\bar{\eta}_a$ is a parameter reflecting traveler's risk perception of safety variance for segment a at speed v_a. Thus, the variance of CRC distribution of the segment link a is expressed as:

$$ {\sigma_a}^2 = {t_a}^2 \bar{\gamma} {v_a}^{\bar{\eta}_a} \tag{8}$$

(4) CRC distribution of intersection

Intersections are hazardous locations on the transport network because of the crossing traffic streams (Xie et al., 2014; Xu et al., 2014c; Huang et al., 2017). It is estimated that nearly 45% of all crashes and 23% of crashes with fatalities occur at or near intersections throughout the United States (Bagloee and Asadi, 2016). Rather than representing the intersection as a simple node, it is more accurate to separately model each movement type (turning or crossing) at an intersection. The CRC distribution of intersection movement $a \to b$ is expressed as:

$$r_{a\to b} \sim Dist_2\left(E(r_{a\to b}), {\sigma_{a\to b}}^2\right) \qquad \forall a \to b \in \bar{A} \tag{9}$$

where $r_{a\to b}$ denotes the CRC of an intersection movement $a \to b$; $E(r_{a\to b})$ is the corresponding mean CRC, and $\sigma_{a\to b}$ is the standard deviation.

Moreover, different movements on an intersection have different hazard levels depending on the different number of conflicts created by competing traffic streams. Left-turning traffic, for example, is a major source of conflicts at intersections, accounting for approximately 45% of all intersection crashes. However, travelers usually spend only a short time in an intersection, and there is no significant difference between various turning movements in terms of the duration or the speed of travel. Therefore, the frequency of the conflicts is closely related to the traffic volume, which is a relatively reliable proxy for exposure to indicate the crash risk of different turnings. Thus, in this study, we quantify the CRC of each movement type at intersections with regard to the traffic volume. Accordingly, the mean and variance of the CRC distribution of turning link $a \to b$ can be expressed as:

$$E(r_{a\to b}) = \tau g(x_{a\to b}) \tag{10}$$

$$ {\sigma_{a\to b}}^2 = \bar{\tau} \bar{g}(x_{a\to b}) \tag{11}$$

where $x_{a\to b}$ is the traffic volume on turning link $a \to b$; τ and $\bar{\tau}$ are adjustment coefficients; and $g(\cdot)$ and $\bar{g}(\cdot)$ are the functional relationships between the traffic volume and the mean and variance of the CRC distribution, respectively. McDonald (1953), in early research, found a certain exponential relation (as shown in Fig. 4) between traffic volume and intersection safety by investigating the crashes at 150 intersections. Therefore, the volume-safety relations, as perceived by travelers, for different movements at intersections can be represented by a power function. In this function, the exponent parameter can be set to various values to account for the variation of travelers' perceptions of the hazard-level of different intersection movements. Consequently, Eq. (10) and Eq. (11) can be expressed as:

$$E(r_{a\to b}) = \tau {x_{a\to b}}^{\omega_{a\to b}} \tag{12}$$

$$ {\sigma_{a\to b}}^2 = \bar{\tau} {x_{a\to b}}^{\bar{\omega}_{a\to b}} \tag{13}$$

where $\omega_{a\to b}$ and $\bar{\omega}_{a\to b}$ are variable parameters reflecting the perceived hazard-level of different intersection movements, whose values are both assumed to be lower than 1.

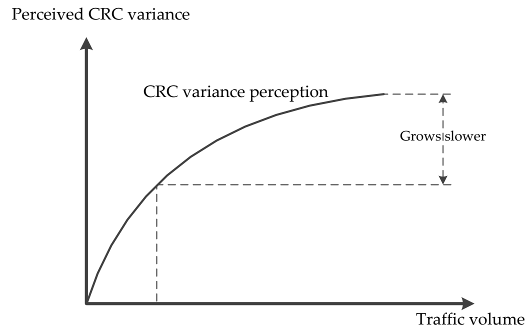

Fig. 4 Relationship between CRC and traffic volume at intersection

Note that, as shown in Fig. 4, because the value of $\omega_{a\to b}$ and $\bar{\omega}_{a\to b}$ are both below 1, the perceived crash risk grows more slowly as a function of traffic volume as the traffic volume increases. This relationship captures the widely reported empirical phenomenon that the crash risk at an intersection increases more slowly as the number of vehicles growth (Geyer et al., 2006).

(5) Route CRC distribution

On the basis of the CRC distribution of road segment and intersection turning movement, the route CRC variable can be expressed by summing the corresponding link (road sites) CRC variables:

$$r_p = \sum_{a\in A} r_a \delta_a^p + \sum_{a\to b\in \bar{A}} r_{a\to b}\, \delta_{a\to b}^p \tag{14}$$

where r_p is the CRC of route p. δ_a^p is the route-link incidence parameter whose value is one if a is on p; zero otherwise. Similarly, $\delta_{a\to b}^p$ is the route-turn incidence parameter whose value is one if $a\to b$ is on p; zero otherwise.

This study assumes that the link CRC distributions (of segments and intersection movements) in the road network are independent and bounded with finite and non-zero variance. Regardless of the link and turn CRC distribution, as long as the distributions are independent and bounded with finite and non-zero variance, the route CRC follows a normal distribution according to the Central Limit Theorem (Lo et al., 2006). Thus, the route CRC mean and standard deviation may be assumed as:

$$\begin{gathered} r_p \sim N(E(r_p), {\sigma_p}^2) \\ E(r_p) = \sum_{a\in A}[\delta_a^p \cdot E(r_a)] + \sum_{a\to b\in \bar{A}}[\delta_{a\to b}^p \cdot E(r_{a\to b})] \\ \sigma_p = \sqrt{\sum_{a\in A}[\delta_a^p \cdot {\sigma_a}^2] + \sum_{a\to b\in \bar{A}}[\delta_{a\to b}^p \cdot {\sigma_{a\to b}}^2]} \end{gathered} \tag{15}$$

where $E(r_p)$ is the mean CRC of route p and σ_p is the standard deviation of the CRC of route p.

2.2 Definition of effective CRC

In the transportation literature, Jackson and Jucker (1982) introduced a framework from the view of travel reliability. It assumes that traveler looks to maximize the option's return (minimize the cost of the choice) while minimize its associated risk/uncertainty. The option's return is represented by the expected value, and the risk/uncertainty by the variance[1]. Most studies that try to model traveler's travel time reliability concerns, such as Uchida and Iida (1993), Lo and Tung (2003), Lo et al. (2006) and Ni (2011), Chen et al. (2010 and 2011), Xu et al. (2017) and Xu et al. (2018), are basically built on this theoretical framework. This framework prescribes how travelers deal with unreliable prospects based on distinct states of nature of each alternative, and represents the states by a distribution of outcomes (Carrion and Levinson, 2012). In this framework, it is assumed that the traveler has a priori information of the mean and variance of the nature of each alternative in their choice set within a category. In the context of travel

[1] This framework is developed on the basis of risk-return model in finance (see Markowitz (1999) for an overview) and the expected utility theory proposed by Von and Morgenstern (1944).

safety reliability, the set of alternatives could be routes between an O-D pair. The states of nature could be extreme weather, mountainous region, bad road surface, hazard conflict and crash. The outcomes are likely to be the distribution of the CRC for each alternative. Next, we will try to reset this framework in the context of travel safety reliability according to the CRC distribution which is specified in above section.

The randomness of crash occurrence causes the variability of the route CRC. With the safety reliability requirements of travelers, they create a larger CRC budget than the expected CRC to hedge against the variability of the CRC. In this study, we define travelers' safety reliability requirement to be ρ. As shown in Fig. 5, it means the probability that the actual trip CRC is within the specified CRC, denoted as R_p. This specific CRC is referred to as the effective crash risk cost (effective CRC):

$$p\{r_p \leq R_p\} = \rho. \qquad (16).$$

For example, in Fig. 6 we present two different routes that have the same mean CRC but perform distinct safety reliabilities. Travelers who have the same higher safety reliability requirement would not prefer to select route 2, because they need to create a larger CRC budget (R_2) if traveling through route 2 to avoid the possible higher loss caused by its lower safety reliability.

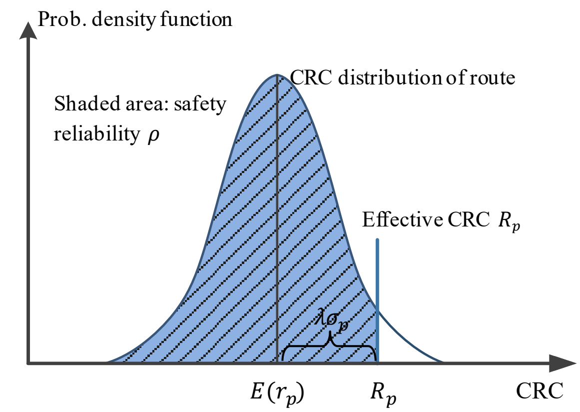

Fig. 5 Within specified safety reliability and effective CRC

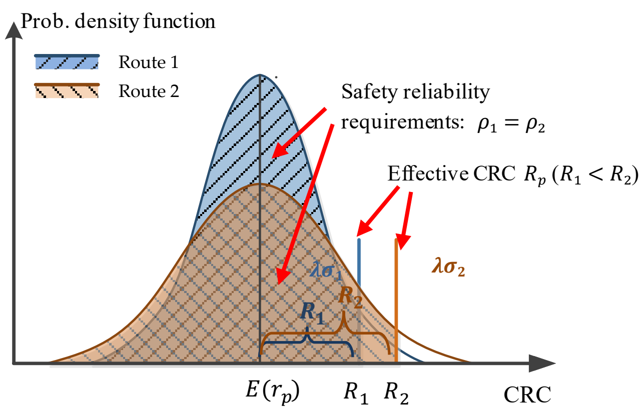

Fig. 6 Two route with same mean CRC but different safety reliabilities

Travelers, in reality, do not exactly know their certain priori risk of being involved in a traffic crash. Their crash risk aversions may vary in different traveler groups. Those travelers who attach great importance to travel safety would add a travel CRC margin to the expected travel CRC, to avoid crash occurrence. Thus, the effective CRC associated with route p can be defined as:

$$[\text{Effective CRC}] = [\text{Expected CRC}] + [\text{CRC Margin}] \qquad (17)$$

and mathematically expressed as:

$$R_p = E(r_p) + \lambda\sigma_p \qquad \forall p \in P_w, \forall w \in W \qquad (18)$$

where λ is the parameter related to the requirement on safe reliability. $\lambda\sigma_p$ denotes the added travel CRC margin, r_p represents the CRC of route p which is a random variable, $E(r_p)$ and σ_p are the mean and standard deviation of r_p. The relation between the safety reliability and the effective CRC is clearly showing in Fig. 5. Obviously, a large λ demonstrates that the traveler has a greater aversion for crash risk and vice versa. They would allow for a larger effective CRC so as to maintain their safety reliability at a high level. Thus, λ is the indicator of representing the degree of risk aversion of travelers.

Then, combining Eq. (16) and Eq. (18), the relation between the effective CRC and safety reliability can be obtained as the following (as shown in Fig. 5):

$$p\{r_p \leq R_p = E(r_p) + \lambda\sigma_p\} = \rho. \qquad (19)$$

By rearranging terms, the (16) can be transformed as:

$$p\left\{\frac{r_p - E(r_p)}{\sigma_p} \leq \lambda\right\} = \rho. \tag{20}$$

We set $s_p = \frac{r_p - E(r_p)}{\sigma_p}$, then s_p is the standard normal variate of r_p, from which it can be deduced that the value λ is determined by ρ.

2.3 Route choice model

In general, travelers with different degrees of crash risk aversions exist in a road network. Hypothesize that there are M classes of travelers in a network, and m labels their different degrees of crash risk aversion. For the travelers of class m with the safety reliability requirement ρ^m, the effective CRC R_p^m follows from Eq. (18) with the corresponding value λ^m:

$$R_p^m = E(r_p) + \lambda^m \sigma_p \qquad \forall p \in P_w, \forall w \in W \tag{21}$$

Undoubtedly, in reality, travelers take into account both road safety and travel time to choose the optimal route. Therefore, the generalized travel cost consists of the travel CRC and the travel time (which is calculated by the BPR function):

$$C_p^m = R_p^m + \theta T_p \tag{22}$$

where θ is cost converting factor of travel time. Similarly, the route travel time variable equals to the total travel time variable of corresponding links:

$$T_P = \sum_{a \in A} (t_a \delta_a^p) \tag{23}$$

Accordingly, the long-term habitual equilibrium route choice pattern of the class m travelers can be stated as: Their flow f_p^m on route p is positive if the generalized travel cost on route p is equal and minimal; all unused routes have an equal or higher generalized travel cost. This equilibrium flow pattern can be expressed by the complementarity conditions as follows:

$$\begin{aligned} &f_p^m (C_p^m - \mu_w^m) = 0 && \forall p \in P_w, \forall w \in W \\ &C_p^m \geq \mu_w^m && \forall p \in P_w, \forall w \in W \end{aligned} \tag{24}$$

where C_p^m is the generalized cost of class m travelers on route p; μ_w^m is the minimum generalized cost of class m travelers among all the routes linking O-D pair w.

The complementarity conditions (24) can be extended to cover a mixed-equilibrium pattern among these different classes. We model this mixed-equilibrium problem with the following mathematical program as:

$$min\ f = \sum_{m=1}^{M} \sum_{w \in W} \sum_{p \in P_w} f_p^m (C_p^m - \mu_w^m) \tag{25}$$

$$\text{s.t. } \sum_{p \in P_w} f_p^m = q_w^m \qquad \forall w \in W, \qquad \forall m = 1, \dots, M \tag{26}$$

$$x_a = \sum_{m=1}^{M} \sum_{w \in W} \sum_{p \in P_w} f_p^m \delta_a^p \qquad \forall a \in A \tag{27}$$

$$x_{a \to b} = \sum_{m=1}^{M} \sum_{w \in W} \sum_{p \in P_w} f_p^m \delta_{a \to b}^p \qquad \forall a \to b \in \bar{A} \tag{28}$$

$$C_p^m - \mu_w^m \geq 0 \qquad \forall m = 1, \dots, M \tag{29}$$

$$f_p^m \geq 0, \mu_w^m \geq 0 \qquad \forall p \in P_w, \forall w \in W, \quad \forall m = 1, \dots, M \tag{30}$$

The parameter q_w^m is the O-D demand for user class m on O-D pair w; x_a is the flows of link a; $x_{a \to b}$ is the flow of intersection turning movement $a \to b$ at intersections. The function f refers to the overall gap to capture the complementarity conditions for the M classes of travelers as in Eq. (24). Constraint (26) represents the relationship between route flow and demand conservation condition for class m travelers on O-D pair w. Constraints (27) and (28) convert the route flows into link flows x_a and $x_{a \to b}$ through the route-link incident indictor δ_a^P and $\delta_{a \to b}^P$ respectively.

3. MODEL SOLUTION ALGORITHM

As the route cost is non-additive with arc costs for the reason that the standard deviation of the effective travel cost on a route is route-specific and not equal to the sum of the standard deviations of the arc cost, the above passenger assignment model should be route-based, and cannot be translated into a link-based model (Gabriel and Bernstein, 1997). Thus, we also let the algorithm for solving the passenger assignment model be route-based. Lo and Chen (2000) proposed a route-based algorithm for solving the traffic equilibrium problem with route-specific cost. Similarly, we use the k-shortest route algorithm to find k-lowest mean travel cost routes and generate a route subset. The minimum effective CRC route can be solved in the obtained route set for each O-D pair. In each iteration, the All-or-Nothing (AON) assignment is applied to load the passenger demand. In the solving algorithm, the method of successive averages (MSA) is adopted to determine the step size. The details of the algorithmic steps are described as follows:

Step 1: initialization

- Initialize parameters and variables: the degree of risk aversion of class m travelers, λ^m; impedance parameters, α and β; the free-flow travel time t_a^0; the capacity of link a, c_a; conversion coefficient, θ; the stopping tolerance, ε; the demand of class m travelers between O-D pair w, q_w^m.
- Set iteration counter $n \leftarrow 1$
- Let $x_a^n \leftarrow 0$; $x_{a\to b}^n \leftarrow 0$; initial route set $\bar{P}_w \leftarrow \emptyset$.

Step 2: update route flow

- Compute the expected CRC of links, i.e., $E(r_a)$ and $E(r_{a\to b})$, and travel times of links t_a.
- Compute link costs: $C_a \leftarrow E(r_a) + \theta T_a$ and $C_{a\to b} \leftarrow E(r_{a\to b})$.
- Compute the k-shortest route set $\hat{P}_w$ with the above link costs C_a and $C_{a\to b}$ using the k-shortest route algorithm.
- Compute the generalized travel costs C_p^m for $p \in \hat{P}_w$ and each class $m = 1, \dots, M$.
- Obtain the shortest route in the obtained shortest route set $p_w^m \leftarrow arg\ min\, \{C_p^m | p \in \hat{P}_w\}$, and update the route set $\bar{P}_w = \bar{P}_w \cup p_w^m$ for each class $m = 1, \dots, M$.
- Perform AON assignment: load the demand q_w^m to route p_w^m, i.e. for each route $p \in \bar{P}_w$, if $p = p_w^m$, let $h(p_w^m) \leftarrow q_w^m$; otherwise, let $h(p_w^m) \leftarrow 0$.
- Update route flow $f_p^m \leftarrow \frac{n-1}{n} f_p^m + \frac{1}{n} h(p)\ \ \forall p \in \bar{P}_w, \forall w \in W, \forall m \in M$.

Step 3: Update links and nodes flow

- Update the main iteration counter $n \leftarrow n + 1$.
- Calculate the arc flow $x_a^n \leftarrow \sum_{m=1}^{M} \sum_{w\in W} \sum_{p\in \bar{P}_w} f_p^m \delta_a^p$.
- Calculate the turning flow $x_{a\to b}^n \leftarrow \sum_{m=1}^{M} \sum_{w\in W} \sum_{p\in \bar{P}_w} f_p^m \delta_{a\to b}^p$.

Step 4: Check convergence

- If $\frac{\sqrt{\sum_{a\in A}(x_a^n - x_a^{n-1})^2 + \sum_{a\to b\in \bar{A}}(x_{a\to b}^n - x_{a\to b}^{n-1})^2}}{\sum_{a\in A} x_a^{n-1} + \sum_{a\to b\in \bar{A}} x_{a\to b}^{n-1}} < \varepsilon$, then terminate, otherwise repeat the step 2.

For solving the large-scale networks, it will take much calculating time to use the k-shortest route algorithm for finding k-lowest mean travel cost routes in each iteration. In the real cases, the number of routes chosen by the users may be limited for each O-D pair. Consequently, for saving the calculating time, we can find a route subset in the initialization step and replace the whole route set with it for each O-D pair. It saves the process of computing the k-shortest route set in Step 2. It is obvious that the method of choosing this route subset will affects the solution. The k-shortest route algorithm (Xu et al., 2018) and the penalty method (De La Barra et al., 1993) can be used to choose this route subset. For further improving the efficiency of the algorithm, a self-regulated averaging method can be adopted to determine the step size (Liu et al., 2009).

4. NUMERICAL STUDIES

4.1 A toy network: Nguyen and Dupuis' network

The formulations are firstly applied to a test network called the Nguyen and Dupuis fall network for demonstrating its application. As shown in Fig. 7, the network consists of 13 nodes, 19 links and 4 O-D pairs. Letter a_n is the code of each link. Definitions of intersection movements in each node are shown in Table 1. The free-flow travel time, design capacity values, the length of each road segment and traveler's risk perceptions related to segment features and driving speed are shown in Table 2. The values of adjustment coefficients in Eq. (12) and Eq. (13) are predefined in Table 3 according to the type of turning movement with different hazard level. The demands of the O-D pair (1,2), (1,3), (4,2), (4,3) are 400, 800, 600, 200 pcu/h, respectively. The unit crash risk evaluation functions and safety reliability evaluation functions are as shown in (6), (8) and (12), (13), with γ =3×10^{-4}, $\bar{\gamma}$ =7×10^{-5}, τ =5×10^{-3} and $\bar{\tau}$ =5×10^{-4}. The parameters of link generalized cost function and performance function are α=0.15, β=4 and θ=3, respectively.

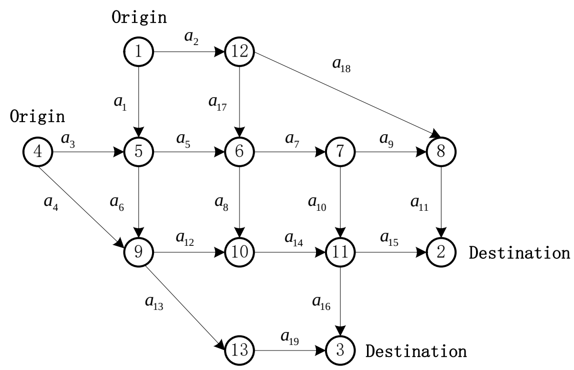

Fig. 7 Nguyen and Dupuis' network

Table 1 Definition on Each Turn in Nguyen and Dupuis Network

Movement	Definition
Left-turn	$a_1 \to a_5$, $a_6 \to a_{12}$, $a_8 \to a_{14}$, $a_{10} \to a_{15}$, $a_{17} \to a_7$
Crossing	$a_1 \to a_6$, $a_2 \to a_{18}$, $a_3 \to a_5$, $a_4 \to a_{12}$, $a_4 \to a_{13}$, $a_5 \to a_7$, $a_6 \to a_{13}$, $a_7 \to a_9$, $a_{10} \to a_{16}$, $a_{12} \to a_{14}$, $a_{13} \to a_{19}$, $a_{14} \to a_{15}$, $a_{17} \to a_8$, $a_{18} \to a_{11}$
Right-turn	$a_2 \to a_{17}$, $a_3 \to a_6$, $a_5 \to a_8$, $a_7 \to a_{10}$, $a_9 \to a_{11}$, $a_{14} \to a_{16}$

Table 2 Nguyen and Dupuis Network Parameters

Link	t_a^0 / min^{-1}	c_a/(pcu h^{-1})	Length (km)	η_a	$\bar{\eta}_a$	Link	t_a^0/ min^{-1}	c_a/(pcu h^{-1})	Length (km)	η_a	$\bar{\eta}_a$
a_1	7	800	5	2.1	2.6	a_{11}	9	550	5	2.1	2.6
a_2	9	400	5	2.1	2.6	a_{12}	10	550	5	2	2.5
a_3	9	200	5	2.1	2.6	a_{13}	9	600	5	2.1	2.6
a_4	12	800	5	2	2.5	a_{14}	6	700	5	2.1	2.6
a_5	3	350	5	2.2	2.7	a_{15}	9	500	5	2.1	2.6
a_6	9	400	5	2.1	2.6	a_{16}	8	300	5	2.1	2.6
a_7	5	800	5	2.2	2.7	a_{17}	7	200	5	2.1	2.6
a_8	13	250	5	2	2.5	a_{18}	14	400	5	2	2.5
a_9	5	250	5	2.2	2.7	a_{19}	11	600	5	2	2.5
a_{10}	9	300	5	2.1	2.6	-	-	-	-	-	-

Table 3 CRC Parameters of Intersection Turns

Movement	$\omega_{a\to b}$	$\bar{\omega}_{a\to b}$
Left-turn	0.5	0.8
Crossing	0.4	0.6
Right-turn	0.25	0.4

Four cases are discussed in this study. Two types of travelers are considered, including low reliability (LR) class travelers, who set the effective CRC to be simply the mean trip CRC (λ=0, ρ=0.5), and high reliability (HR) class travelers, who reserve a large effective CRC of 95% (λ=1.64, ρ=0.95). In the first three cases, we consider that there exists only one type of traveler in the entire network: either LR or HR. The travel cost in these three cases, respectively, are only considering: (1) the travel time; (2) both the travel time and the travel CRC of links and nodes; and (3) the travel time and the travel CRC of only links. In the last case, (4) both types of travelers are considered in the network and are evenly split, with half LR travelers and half HR travelers. The travel cost includes the travel time and the travel CRC of links and nodes. The assumptions of each case are shown in Table 4.

Table 4 Assumptions of Four Cases

Cases	Generalized travel cost	Traveler class
1	Travel time	Single-class travelers
2	Travel time, CRC of links and nodes	Single-class travelers
3	Travel time, CRC of links	Single-class travelers
4	Travel time, CRC of links and nodes	Multi-class travelers

4.1.1 Single-class travelers

In Table 5, the travel time on all utilized routes of each O-D pair is equal and minimal, which indicates that the equilibrium state is achieved. In the following section, the O-D pair (1, 3) is used for analyzing the equilibrium state of other cases when changing the assumptions.

Table 5 Traffic Equilibrium Results with Considering Travel Time Only

O-D pair	Route	Link sequence	Route time/min	Route flow/ $\left(pcu\cdot h^{-1}\right)$
(1,2)	1	$\{a_1, a_1\to a_5, a_5, a_5\to a_7, a_7, a_7\to a_9, a_9, a_9\to a_{11}, a_{11}\}$	36.50	27.22
	2	$\{a_1, a_1\to a_5, a_5, a_5\to a_7, a_7, a_7\to a_{10}, a_{10}, a_{10}\to a_{15}, a_{15}\}$	41.68	0.00
	3	$\{a_1, a_1\to a_5, a_5, a_5\to a_8, a_8, a_8\to a_{14}, a_{14}, a_{14}\to a_{15}, a_{15}\}$	43.55	0.00
	4	$\{a_1, a_1\to a_6, a_6, a_6\to a_{12}, a_{12}, a_{12}\to a_{14}, a_{14}, a_{14}\to a_{15}, a_{15}\}$	45.14	0.00
	5	$\{a_2, a_2\to a_{17}, a_{17}, a_{17}\to a_7, a_7, a_7\to a_9, a_9, a_9\to a_{11}, a_{11}\}$	38.65	0.00
	6	$\{a_2, a_2\to a_{17}, a_{17}, a_{17}\to a_7, a_7, a_7\to a_{10}, a_{10}, a_{10}, \to a_{15}, a_{15}\}$	43.81	0.00
	7	$\{a_2, a_2\to a_{17}, a_{17}, a_{17}\to a_8, a_8, a_8\to a_{14}, a_{14}, a_{14}\to a_{15}, a_{15}\}$	45.68	0.00
	8	$\{a_2, a_2\to a_{18}, a_{18}, a_{18}\to a_{11}, a_{11}\}$	36.50	372.78
(1,3)	**9**	$\{a_1, a_1\to a_5, a_5, a_5\to a_7, a_7, a_7\to a_{10}, a_{10}, a_{10}\to a_{16}, a_{16}\}$	**42.79**	**366.32**
	10	$\{a_1, a_1\to a_5, a_5, a_5\to a_8, a_8, a_8\to a_{14}, a_{14}, a_{14}\to a_{16}, a_{16}\}$	**44.66**	**0.00**
	11	$\{a_1, a_1\to a_6, a_6, a_6\to a_{12}, a_{12}, a_{12}\to a_{14}, a_{14}, a_{14}\to a_{16}, a_{16}\}$	**46.26**	**0.00**
	12	$\{a_2, a_2\to a_{17}, a_{17}, a_{17}\to a_7, a_7, a_7\to a_{10}, a_{10}, a_{10}\to a_{16}, a_{16}\}$	**44.92**	**0.00**
	13	$\{a_2, a_2\to a_{17}, a_{17}, a_{17}\to a_8, a_8, a_8\to a_{14}, a_{14}, a_{14}\to a_{16}, a_{16}\}$	**46.80**	**0.00**
	14	$\{a_1, a_1\to a_6, a_6, a_6\to a_{13}, a_{13}, \quad a_{13}\to a_{19}, a_{19}\}$	**42.79**	**433.68**
(4,2)	15	$\{a_3, a_3\to a_5, a_5, a_5\to a_7, a_7, a_7\to a_9, a_9, a_9\to a_{11}, a_{11}\}$	38.65	199.31
	16	$\{a_3, a_3\to a_5, a_5, a_5\to a_7, a_7, a_7\to a_{10}, a_{10}, a_{15}\to a_{15}, a_{15}\}$	43.81	0.00
	17	$\{a_3, a_3\to a_5, a_5, a_5\to a_8, a_8, a_8\to a_{14}, a_{14}, a_{14}\to a_{15}, a_{15}\}$	45.68	0.00
	18	$\{a_3, a_3\to a_6, a_6, a_6\to a_{12}, a_{12}, a_{12}\to a_{14}, a_{14}, a_{14}\to a_{15}, a_{15}\}$	47.28	0.00

	19	$\{a_4, a_4 \to a_{12}, a_{12}, a_{12} \to a_{14}, a_{14}, a_{14} \to a_{15}, a_{15}\}$	38.65	400.69
(4,3)	20	$\{a_3, a_3 \to a_5, a_5, a_5 \to a_7, a_7, a_7 \to a_{10}, a_{10}, a_{16} \to a_{16}, a_{16}\}$	44.93	0.00
	21	$\{a_3, a_3 \to a_5, a_5, a_5 \to a_8, a_8, a_8 \to a_{14}, a_{14}, a_{14} \to a_{16}, a_{16}\}$	46.80	0.00
	22	$\{a_3, a_3 \to a_6, a_6, a_6 \to a_{12}, a_{12}, a_{12} \to a_{14}, a_{14}, a_{14} \to a_{16}, a_{16}\}$	48.39	0.00
	23	$\{a_3, a_3 \to a_6, a_6, a_6 \to a_{13}, a_{13}, a_{13} \to a_{19}, a_{19}\}$	44.92	0.00
	24	$\{a_4, a_4 \to a_{12}, a_{12}, a_{12} \to a_{14}, a_{14}, a_{14} \to a_{16}, a_{16}\}$	39.77	0.00
	25	$\{a_4, a_4 \to a_{13}, a_{13}, a_{13} \to a_{19}, a_{19}, a_{19}\}$	36.30	200.00

#Bold number is the focused route in this study

Table 6 depicts the route flow results for the LR and HR route choice models considering both travel time and the travel CRC. It shows that comparing the result with case 1, when considering the CRC of links and nodes, the route choice model allocates a different amount of flow to the routes. Because route 5 and 6 have lower mean CRC ($E(r_p)$), the flows shift from route 1 (which has the highest mean and standard deviation of CRC) to these two relatively safer routes. In addition, as the safest route among six routes, in this case, most amount of flow is allocated on route 5. Further comparing the results between two road choice models, the HR model allocates less flow than the LR model to route 6. This is because route 6 have the highest standard deviations (σ_p) of the CRC comparing with other routes, which means the CRC distributions of route 6 are much more dispersed than other routes. The HR model seriously considers the safety reliability in determining the effective CRC. However, LR travelers are only concerned about mean travel safety and travel time. Thus, HR travelers allocate more flows on route 5 to avoid the links in which crashes are more likely to occur.

Table 6 Traffic Equilibrium Results of LR (HR) travelers (considering link and turning safety)

Route	$E(r_{a\to b})$	$\sigma_{a\to b}$	$E(r_p)$	σ_p	R_p	T_p	C_p	Route flow
1	0.00	0.00	148.92 (148.20)	41.09 (41.01)	148.92 (215.46)	97.90 (99.34)	246.82 (314.80)	0.00 (0.00)
2	0.00	0.00	118.91 (116.41)	37.04 (36.75)	118.91 (176.67)	121.37 (130.48)	240.28 (307.15)	0.00 (0.00)
3	23.54	38.20	80.87 (78.90)	48.53 (46.73)	80.87 (155.54)	151.41 (150.88)	232.27 (306.42)	0.00 (0.00)
4	1.09	3.79	84.33 (79.06)	34.48 (33.84)	84.33 (134.57)	142.67 (163.15)	227.01 (297.72)	0.00 (0.00)
5	4.37	10.02	57.60 (51.49)	30.97 (30.92)	57.60 (102.19)	166.14 (194.29)	223.75 (296.48)	218.58 (281.18)
6	34.98	50.19	70.92 (69.74)	56.03 (51.99)	70.92 (155.01)	152.83 (141.47)	223.75 (296.49)	581.42 (518.82)

Bracketed figures are the HR travelers; the figures without bracket are LR travelers.

The route flow pattern for two route choice models considering travel time cost and travel safety of only links are shown in Table 7. As expected, when ignoring the travel safety of intersections, a large amount of flow shifts from route 5 to route 6. This is because that in case 2 the movements at the intersections seriously influence the travel safety conditions of route 6 (which have the highest mean and standard deviation of the turning CRC). The ignorance of turning safety makes this route seemingly safer, so that attract more travelers. Furthermore, in contrast with case 2, HR travelers allocate more flow to route 6 but lower to route 5 than LR travelers, in order to avoid the dangerous links on route 5 (route 6 is relatively more reliable in safety, i.e. higher σ_p value, than route 5).

Table 7 Traffic Equilibrium Results of LR (HR) travelers (considering only links safety)

Route	The number of intersections	$E(r_p)$	σ_p	R_p	T_p	C_p	Route flow
1	4	149.02	41.10	149.02	97.61	246.63	0.00
		(148.92)	(41.09)	(216.31)	(97.73)	(314.04)	(0.00)
2	4	120.56	37.23	120.56	116.79	237.35	0.00
		(120.89)	(37.26)	(182.00)	(116.09)	(298.09)	(0.00)
3	4	57.12	29.80	57.12	160.39	217.51	0.00
		(56.92)	(29.73)	(105.68)	(164.78)	(270.46)	(0.00)
4	4	87.70	34.86	87.70	129.19	216.89	0.00
		(88.70)	(34.99)	(146.09)	(126.18)	(272.26)	(0.00)
5	4	59.25	30.20	59.25	148.37	207.61	146.24
		(60.67)	(30.40)	(110.53)	(144.54)	(255.07)	(121.02)
6	3	32.46	24.15	32.46	175.15	207.61	653.76
		(31.26)	(23.87)	(70.40)	(184.67)	(255.07)	(678.98)

Bracketed figures are the HR travelers; the figures without bracket are LR travelers.

4.1.2 Multi-class travelers

In this case, we consider that the network consists of two types of travelers forming the mix-equilibrium model. Each type of traveler accounts for half of the total network. Table 8 shows the route flow result. As we can see, the route mean CRC ($E(r_p)$), standard deviation of the route CRC (σ_p) and route travel time (T_p) are consistent for these two type of travelers. All of the LR travelers select route 6, which has the lowest general cost (C_p) between O-D pair (1, 3). By contrast, since the route travel safety dispersions are of concern to the HR travelers, most of them select route 5, which have the highest safety reliability (lowest σ_p) than other routes. This route flow result reflects the nature of route choice behavior that the travelers with higher effective CRC tend to choose more reliable routes.

Table 8 Traffic Equilibrium State of Multi-class Users

Traveler class	Route	$E(r_p)$	σ_p	R_p	T_p	C_p	Route flow
LR model	1	148.20	41.01	148.20	99.34	247.54	0.00
	2	116.41	36.75	116.41	130.48	246.89	0.00
	3	78.90	46.73	78.90	150.87	229.77	0.00
	4	79.06	33.84	79.06	163.15	242.21	0.00
	5	51.49	30.92	51.49	194.29	245.78	0.00
	6	69.75	51.99	69.75	141.47	211.21	400.00
HR model	1	148.20	41.01	215.46	99.34	314.80	0.00
	2	116.41	36.75	176.67	130.48	307.15	0.00
	3	78.90	46.73	155.54	150.87	306.41	0.00
	4	79.06	33.84	134.57	163.15	297.72	0.00
	5	51.49	30.92	102.19	194.29	296.48	281.10
	6	69.75	51.99	155.02	141.47	296.48	118.90

4.2 A real network: Sioux falls network

This case aims to test the proposed route choice model and the algorithm including its feasibility and efficiency for the well-known Sioux falls network (Fig. 8). As shown in Fig. 8, in this case, each node is disintegrated into a set of turns. Consequently, this network consists of 76 nodes and 254 links (including the total number of turn links). There are 528 O-D pairs in this network. The definition of intersection movements in each node and the information of each link are shown in Table 9 and Table 10, respectively. The CRC parameters of different intersection turning movement are the same with those in the example in Section 5.1. The parameters in safety evaluation function, generalized cost function and performance function are $\gamma = 3 \times 10^{-6}$, $\bar{\gamma} = 7 \times 10^{-7}$, $\tau = 5 \times 10^{-5}$, $\bar{\tau} = 5 \times 10^{-6}$ $\alpha = 0.15$, $\beta = 4$ and $\theta = 3$, respectively.

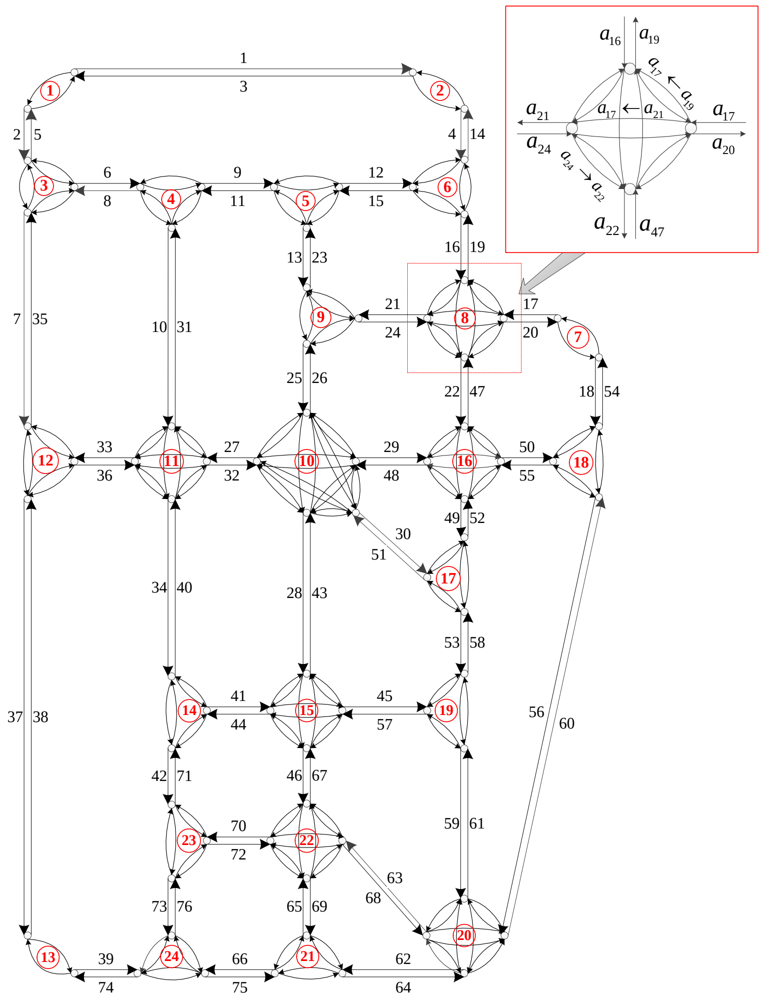

Fig. 8 Sioux falls network

Table 9 Definition on Each Turn in Sioux Falls Network

Nodes	1	2	3	4	5	6	7	8
Left	$a_3 \rightarrow a_2$	$a_{14} \rightarrow a_3$	$a_2 \rightarrow a_6$, $a_8 \rightarrow a_7$	$a_{31} \rightarrow a_8$, $a_{11} \rightarrow a_{10}$	$a_{23} \rightarrow a_{11}$, $a_{15} \rightarrow a_{13}$	$a_{19} \rightarrow a_{15}$, $a_{12} \rightarrow a_{14}$	$a_{54} \rightarrow a_{17}$	$a_{47} \rightarrow a_{21}$, $a_{17} \rightarrow a_{22}$, $a_{16} \rightarrow a_{20}$, $a_{24} \rightarrow a_{19}$
Straight	-	-	$a_2 \rightarrow a_7$, $a_{35} \rightarrow a_5$	$a_{11} \rightarrow a_8$, $a_6 \rightarrow a_9$	$a_{15} \rightarrow a_{11}$, $a_9 \rightarrow a_{12}$	$a_{19} \rightarrow a_{14}$, $a_4 \rightarrow a_{16}$	-	$a_{17} \rightarrow a_{21}$, $a_{24} \rightarrow a_{20}$, $a_{16} \rightarrow a_{22}$, $a_{47} \rightarrow a_{19}$
Right	$a_5 \rightarrow a_1$	$a_1 \rightarrow a_4$	$a_8 \rightarrow a_5$, $a_{35} \rightarrow a_6$	$a_{31} \rightarrow a_9$, $a_6 \rightarrow a_{10}$	$a_9 \rightarrow a_{13}$, $a_{23} \rightarrow a_{12}$	$a_{12} \rightarrow a_{16}$, $a_4 \rightarrow a_{15}$	$a_{20} \rightarrow a_{18}$	$a_{24} \rightarrow a_{22}$, $a_{47} \rightarrow a_{20}$, $a_{17} \rightarrow a_{19}$,

								$a_{16} \to a_{21}$
Nodes	9	10	11	12	13	14	15	16
Left	$a_{21} \to a_{25}$, $a_{13} \to a_{24}$	$a_{32} \to a_{26}$, $a_{43} \to a_{27}$, $a_{48} \to a_{28}$, $a_{25} \to a_{29}$, $a_{48} \to a_{30}$, $a_{51} \to a_{28}$, $a_{25} \to a_{30}$, $a_{51} \to a_{27}$	$a_{36} \to a_{31}$, $a_{40} \to a_{33}$, $a_{27} \to a_{34}$, $a_{10} \to a_{32}$	$a_{7} \to a_{36}$, $a_{33} \to a_{37}$	$a_{37} \to a_{39}$	$a_{34} \to a_{41}$, $a_{44} \to a_{42}$	$a_{28} \to a_{45}$, $a_{41} \to a_{43}$, $a_{67} \to a_{44}$, $a_{57} \to a_{46}$	$a_{29} \to a_{47}$, $a_{52} \to a_{48}$, $a_{55} \to a_{49}$, $a_{22} \to a_{50}$
Straight	$a_{13} \to a_{25}$, $a_{26} \to a_{23}$	$a_{48} \to a_{27}$, $a_{32} \to a_{29}$, $a_{25} \to a_{28}$, $a_{43} \to a_{26}$	$a_{27} \to a_{33}$, $a_{36} \to a_{32}$, $a_{10} \to a_{34}$, $a_{40} \to a_{31}$	$a_{7} \to a_{37}$, $a_{38} \to a_{35}$	-	$a_{34} \to a_{42}$, $a_{71} \to a_{40}$	$a_{41} \to a_{45}$, $a_{57} \to a_{44}$, $a_{28} \to a_{46}$, $a_{67} \to a_{43}$	$a_{29} \to a_{50}$, $a_{55} \to a_{48}$, $a_{52} \to a_{47}$, $a_{22} \to a_{49}$
Right	$a_{26} \to a_{24}$, $a_{21} \to a_{23}$	$a_{25} \to a_{27}$, $a_{32} \to a_{28}$, $a_{43} \to a_{29}$, $a_{48} \to a_{26}$, $a_{51} \to a_{29}$, $a_{43} \to a_{30}$, $a_{51} \to a_{26}$, $a_{32} \to a_{30}$	$a_{10} \to a_{33}$, $a_{36} \to a_{34}$, $a_{40} \to a_{32}$, $a_{27} \to a_{31}$	$a_{33} \to a_{35}$, $a_{38} \to a_{36}$	$a_{74} \to a_{38}$	$a_{44} \to a_{40}$, $a_{71} \to a_{41}$	$a_{57} \to a_{43}$, $a_{28} \to a_{44}$, $a_{41} \to a_{46}$, $a_{67} \to a_{45}$	$a_{22} \to a_{48}$, $a_{29} \to a_{49}$, $a_{52} \to a_{50}$, $a_{55} \to a_{47}$
Nodes	17	18	19	20	21	22	23	24
Left	$a_{30} \to a_{52}$, $a_{58} \to a_{51}$	$a_{50} \to a_{54}$, $a_{60} \to a_{55}$	$a_{45} \to a_{58}$, $a_{61} \to a_{57}$	$a_{68} \to a_{61}$, $a_{64} \to a_{63}$, $a_{56} \to a_{62}$, $a_{59} \to a_{60}$	$a_{75} \to a_{65}$, $a_{69} \to a_{64}$	$a_{72} \to a_{67}$, $a_{65} \to a_{70}$, $a_{46} \to a_{68}$, $a_{63} \to a_{69}$	$a_{42} \to a_{72}$, $a_{70} \to a_{73}$	$a_{73} \to a_{75}$, $a_{39} \to a_{76}$
Straight	$a_{49} \to a_{53}$, $a_{58} \to a_{52}$	$a_{18} \to a_{56}$, $a_{60} \to a_{54}$	$a_{53} \to a_{59}$, $a_{61} \to a_{58}$	$a_{68} \to a_{60}$, $a_{56} \to a_{63}$, $a_{64} \to a_{61}$, $a_{59} \to a_{62}$	$a_{62} \to a_{66}$, $a_{75} \to a_{64}$	$a_{72} \to a_{68}$, $a_{63} \to a_{70}$, $a_{46} \to a_{69}$, $a_{65} \to a_{67}$	$a_{76} \to a_{71}$, $a_{42} \to a_{73}$	$a_{39} \to a_{75}$, $a_{66} \to a_{74}$
Right	$a_{49} \to a_{51}$, $a_{30} \to a_{53}$	$a_{18} \to a_{55}$, $a_{50} \to a_{56}$	$a_{53} \to a_{57}$, $a_{45} \to a_{59}$	$a_{59} \to a_{63}$, $a_{68} \to a_{62}$, $a_{64} \to a_{60}$, $a_{56} \to a_{61}$	$a_{69} \to a_{66}$, $a_{62} \to a_{65}$	$a_{46} \to a_{70}$, $a_{72} \to a_{69}$, $a_{63} \to a_{67}$, $a_{65} \to a_{68}$	$a_{70} \to a_{71}$, $a_{76} \to a_{72}$	$a_{66} \to a_{76}$, $a_{73} \to a_{74}$

Table 10 Sioux Falls Network Parameters

Link	t_a^0 / min-1	c_a/(pcu h^{-1})	η_a	$\bar{\eta}_a$	Length (km)	Link	t_a^0/ min-1	c_a/(pcu h^{-1})	η_a	$\bar{\eta}_a$	Length (km)
a_1	1	2590	2.3	2.6	0.6	a_{39}	0.7	2590	2.1	2.5	0.4
a_2	0.7	2340	2.1	2.5	0.4	a_{40}	0.7	509	2.1	2.5	0.4
a_3	0.1	2590	2.3	2.6	0.6	a_{41}	0.9	488	2.1	2.5	0.5
a_4	0.9	496	2.1	2.5	0.5	a_{42}	0.7	513	2.1	2.5	0.4
a_5	0.7	2340	2.1	2.5	0.4	a_{43}	1	492	2.3	2.6	0.6
a_6	0.7	1711	2.1	2.5	0.4	a_{44}	0.9	1351	2.1	2.5	0.5
a_7	0.7	2340	2.1	2.5	0.4	a_{45}	0.5	513	2	2.4	0.3
a_8	0.7	1711	2.1	2.5	0.4	a_{46}	0.5	1456	2	2.4	0.3
a_9	0.3	1778	2	2.4	0.2	a_{47}	0.9	960	2.1	2.5	0.5

a_{10}	1	491	2.3	2.6	0.6	a_{48}	0.7	505	2.1	2.5	0.4
a_{11}	0.3	1778	2	2.4	0.2	a_{49}	0.3	485	2	2.4	0.2
a_{12}	0.7	495	2.1	2.5	0.4	a_{50}	0.5	523	2	2.4	0.3
a_{13}	0.9	1000	2.1	2.5	0.5	a_{51}	1.4	1968	2.3	2.6	0.8
a_{14}	0.9	496	2.1	2.5	0.5	a_{52}	0.3	499	2	2.4	0.2
a_{15}	0.7	495	2.1	2.5	0.4	a_{53}	0.3	523	2	2.4	0.2
a_{16}	0.3	490	2	2.4	0.2	a_{54}	0.3	482	2	2.4	0.2
a_{17}	0.5	784	2	2.4	0.3	a_{55}	0.5	2340	2	2.4	0.3
a_{18}	0.3	2340	2	2.4	0.2	a_{56}	0.7	1968	2.1	2.5	0.4
a_{19}	0.3	490	2	2.4	0.2	a_{57}	0.5	2340	2	2.4	0.3
a_{20}	0.5	784	2	2.4	0.3	a_{58}	0.3	1456	2	2.4	0.2
a_{21}	1.7	505	2.3	2.6	1	a_{59}	0.7	482	2.1	2.5	0.4
a_{22}	0.9	505	2.1	2.5	0.5	a_{60}	0.7	500	2.1	2.5	0.4
a_{23}	0.9	1000	2.1	2.5	0.5	a_{61}	0.7	2340	2.1	2.5	0.4
a_{24}	1.7	505	2.3	2.6	1	a_{62}	1	500	2.3	2.6	0.6
a_{25}	0.5	1392	2	2.4	0.3	a_{63}	0.9	506	2.1	2.5	0.5
a_{26}	0.5	1392	2	2.4	0.3	a_{64}	1	508	2.3	2.6	0.6
a_{27}	0.9	1000	2.1	2.5	0.5	a_{65}	0.3	506	2	2.4	0.2
a_{28}	1	1351	2.3	2.6	0.6	a_{66}	0.5	523	2	2.4	0.3
a_{29}	0.7	485	2.1	2.5	0.4	a_{67}	0.5	489	2	2.4	0.3
a_{30}	1.4	499	2.3	2.6	0.8	a_{68}	0.9	960	2.1	2.5	0.5
a_{31}	1	491	2.3	2.6	0.6	a_{69}	0.3	508	2	2.4	0.2
a_{32}	0.9	1000	2.1	2.5	0.5	a_{70}	0.7	523	2.1	2.5	0.4
a_{33}	1	491	2.3	2.6	0.6	a_{71}	0.7	500	2.1	2.5	0.4
a_{34}	0.7	488	2.1	2.5	0.4	a_{72}	0.7	492	2.1	2.5	0.4
a_{35}	0.7	2340	2.1	2.5	0.4	a_{73}	0.3	500	2	2.4	0.2
a_{36}	1	491	2.3	2.6	0.6	a_{74}	0.7	508	2.1	2.5	0.4
a_{37}	0.5	2590	2	2.4	0.3	a_{75}	0.5	509	2	2.4	0.3
a_{38}	0.5	2590	2	2.4	0.3	a_{76}	0.3	489	2	2.4	0.2

In this case, both low reliability (LR) class travelers with λ=0.52, ρ=0.7 and high reliability (HR) class travelers with λ=1.28, ρ=0.9 are involved in the network. Also, each type of traveler accounts for half (50%) of the total network. For each O-D pair and each traveler class, we calculate the k-lowest mean travel cost routes, denoted by $\hat{P}_w$, for $k = 10$ and $x_a = 0$ in the initialization step, and then find the route with the smallest effective travel cost from the route set $\hat{P}_w$ in each iteration (before convergence). The algorithms were coded in MATLAB (R2014A) and tested on a PC with Inter® Quad-Core 3.00 GHz processor and 3.00 GB RAM. There are totally 5280 route that generated by k-lowest algorithm for each user class, and the total CPU times is 3.92s with $\varepsilon = 10^{-3}$and 38.31s with $\varepsilon = 10^{-4}$.

Table 11 Traffic Equilibrium State of Multi-class Users

O-D pair	Route	$E(r_p)$	σ_p	T_p	LR model		HR model	
					C_p	Route flow	C_p	Route flow

(10, 4)	**1**	**4.00**	**31.45**	**6.47**	**26.82**	**600.00**	**50.73**	**0.00**
	2	**2.12**	**7.91**	**20.62**	**26.85**	**0.00**	**32.87**	**600.00**
	3	3.97	32.22	37.84	58.57	0.00	83.06	0.00
	4	5.22	25.62	27.21	45.75	0.00	65.22	0.00
	5	6.53	40.42	31.44	58.99	0.00	89.71	0.00
	6	10.03	30.35	22.20	48.01	0.00	71.08	0.00
	7	5.33	14.71	42.62	55.60	0.00	66.78	0.00
	8	6.04	34.02	40.52	64.25	0.00	90.11	0.00
	9	14.00	23.86	35.88	62.28	0.00	80.42	0.00
	10	4.45	23.87	64.72	81.58	0.00	99.71	0.00
(10, 5)	**1**	**2.48**	**22.41**	**5.54**	**19.68**	**500.00**	**36.71**	**246.27**
	2	**2.65**	**9.77**	**21.56**	**29.28**	**0.00**	**36.71**	**253.73**
	3	2.81	23.53	36.91	51.95	0.00	69.83	0.00
	4	5.37	33.90	30.51	53.50	0.00	79.26	0.00
	5	8.86	20.89	21.27	41.00	0.00	56.88	0.00
	6	6.39	33.97	28.15	52.21	0.00	78.02	0.00
	7	4.87	25.94	39.60	57.95	0.00	77.67	0.00
	8	5.86	15.79	43.56	57.63	0.00	69.62	0.00
	9	12.48	9.06	34.95	52.14	0.00	59.03	0.00
	10	7.11	33.17	33.20	57.56	0.00	82.76	0.00
(10, 6)	1	1.30	14.39	32.39	41.17	0.00	52.11	0.00
	2	**3.15**	**22.88**	**10.09**	**25.14**	**400.00**	**42.53**	**0.00**
	3	3.86	28.33	25.99	44.58	0.00	66.11	0.00
	4	**7.36**	**9.49**	**16.75**	**29.04**	**0.00**	**36.26**	**400.00**
	5	3.92	22.61	26.11	41.79	0.00	58.97	0.00
	6	3.37	18.06	35.07	47.83	0.00	61.56	0.00
	7	6.96	35.83	36.11	61.70	0.00	88.93	0.00
	8	5.61	27.45	28.67	48.56	0.00	69.42	0.00
	9	6.24	39.16	45.04	71.65	0.00	101.41	0.00
	10	9.20	41.36	29.71	60.42	0.00	91.86	0.00
(10, 7)	1	2.14	17.36	17.64	28.81	0.00	42.00	0.00
	2	**1.15**	**7.02**	**29.02**	**33.82**	**0.00**	**39.16**	**661.93**
	3	3.89	15.88	20.33	32.48	0.00	44.55	0.00
	4	**7.84**	**14.01**	**13.39**	**28.51**	**950.00**	**39.16**	**288.07**
	5	4.75	32.06	20.19	41.61	0.00	65.98	0.00
	6	4.52	32.13	36.70	57.92	0.00	82.34	0.00
	7	3.21	12.98	31.71	41.67	0.00	51.54	0.00
	8	7.48	34.78	21.36	46.93	0.00	73.37	0.00
	9	7.54	33.62	18.02	43.04	0.00	68.59	0.00
	10	5.71	28.92	32.22	52.97	0.00	74.95	0.00

Due to the limited length that is impossible to touch on all the O-D pairs in this network, parts of the O-D pairs which originate from node 10 are selected for analyzing the equilibrium state. Table 11 shows the route flow results of the O-D pairs that present different equilibrium state for two types of travelers. It is consistent with case 4 on the toy network that the route mean CRC ($E(r_p)$), standard deviation of the route CRC (σ_p) and route travel time (T_p) are consistent for these two type of travelers. However, due to the higher concerns of travel safety dispersions, HR travelers select the routes that have relatively lower travel safety standard deviation. For example, between O-D pair 10 and 4, all HR travelers select route 2 which is more reliable in safety than other routes. Also, all HR travelers select the most reliable route in safety—route 4—between node 10 and node 6. Again, it reflects the nature of route choice behavior that the travelers with higher effective CRC tend to choose more reliable routes. It also validates the proposed model and confirms the feasibility and efficiency of algorithm for the real network.

5. CONCLUSION

5.1 Summary

The present study proposes a route choice model for multi-class travelers, which considered both travelers' travel safety concern, i.e. route safety reliability, and travel time concern. The relation between travel safety variability and traveler's route choice behavior is innovatively established. Due to the random nature of crash occurrence, the travel crash risk cost (CRC) of each link (including the dummy links) is described as a distribution. It is assumed that travelers evaluate the travel CRC of a route considering the variability of the route CRC with their safety requirements and factor such information into their route choice consideration in the form of an effective CRC. This effective CRC reflects the degree of the traveler's crash risk aversions. A mixed-equilibrium mathematical program is formulated to describe this route choice behavior of multiple classes of travelers. Two networks including Nguyen and Dupuis' network and Sioux falls network are used to demonstrate the formulations. It is found that (1) the route choice behavior is sensitive to the route safety performance, including route average travel safety and route travel safety variability; (2) the travel safety of intersections would significantly influence the traveler's route choice decision; and (3) travelers with different effective CRC (crash risk aversions) would have different route choice decisions: The HR travelers are strict with route travel safety variability, whereas the LR travelers consider only the route average CRC in their determinations.

5.2 Implications

The proposed traffic assignment method has a great potential for traffic planners and managers in network analysis and in making safety-related policies or regulations. First, this method provides a safety-based travel behavior modeling tool for accommodating the increasing safety demands of travelers. This implies possible new opportunities for transportation planners and managers to reshape travel and activity patterns on both the planning and operational levels when taking into account the impact of road safety on travelers' travel behavior. It will be very useful especially in the upcoming era of intelligent connected vehicles in which abundant in-vehicle safety-related information will be presented to travelers. Second, this method can further be adopted to scientifically and systematically assess the effects of proposed traffic safety policies or regulations on network equilibrium in advance. Depending on an estimation of travelers' behavioral responses[2] to the proposed safety countermeasures, the possible changes of traffic circulation and the corresponding effects on the road network could be clearly specified. This could be helpful for the traffic planners and operators to formulate traffic policies and regulations in a scientific way, beyond making the decisions on the basis of past experience.

5.3 Extension to conflict-based CRC evaluation

In section 3, the traffic volume is applied as a proxy to evaluate the crash risk of turning and crossing movements at intersections and to shape its CRC distribution. In fact, for an intersection movement,

[2] For example, a stricter safety policy or a more effective safety education project would enhance public safety awareness, and thus could further change their travel behaviors.

conflicts with traffic flows from other directions are the significant causes of the high crash risk and thus are highly associated with the shape of the CRC distribution. At an intersection, the number of conflicts is decided by its configuration and geometric features, and the frequency of conflicts occurring along a traffic stream is related to the volume of passing traffic. For example, as shown in Fig. 9, for a four-legged intersection, the left-turn flow ($x_{a_1 \to a_4}$) is not only in conflict with four automobile streams (the crossing flow ($x_{a_3 \to a_8}$), the left-turn flow ($x_{a_3 \to a_6}$), the left-turn flow ($x_{a_7 \to a_2}$), and the crossing flow ($x_{a_5 \to a_2}$)), but also competes with the potential streams of other types of traffic modes (e.g. pedestrian movements).

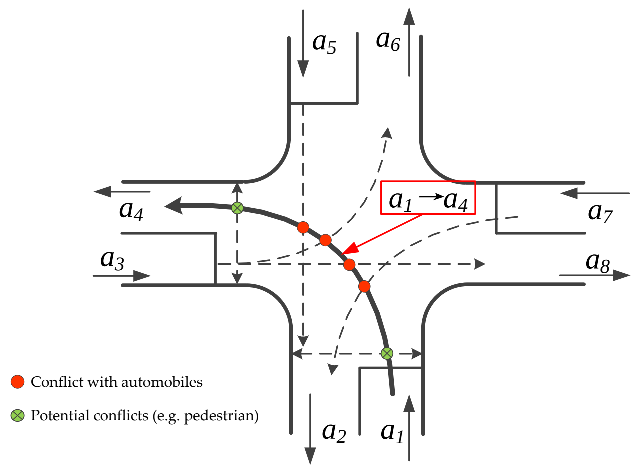

Fig. 9 Conflicts faced by flow in turning $a \to d$ at a four-legged intersection

However, due to a dearth of studies, there is no a well-founded equation that can be used in this study to represent the conflict-CRC relations of different intersection types. Moreover, considering the interactions of flows with different traffic volumes would cause a significant increase in the complexity of computing. Therefore, in this study, the CRC of each intersection movement is estimated simply by accounting for the risk effect posed by the traffic volume along one traffic stream, with the aim of ensuring high computational efficiency. If a reliable function for the relationship between conflicts and the CRC (i.e. $E(r_{a \to d}) = f(x_{a_3 \to a_8}, x_{a_3 \to a_6}, x_{a_7 \to a_2}, x_{a_5 \to a_2})$) was available, Eq. (10) and (11) in proposed model could be replaced to enable the model to account for the effect of flow-related conflicts more explicitly. Meanwhile, an effective algorithm, that can handle the link interactions with an asymmetric CRC, would be essential to solve the resulting conflict-based route choice model (Dafermoss, 1982; Fisk and Nguyen, 1982). These extensions can be accommodated in further by modifying the proposed model and algorithm.

5.4 Limitations and Future researches

To the best of our knowledge, there is no exclusive research that has been performed for modeling traveler's safety-concern route choice behavior. This study fills this gap by developing a route choice model for multi-class travelers both accounting their safety and time concern, which will help the transportation planners and managers to better understand the travelers' safety-concern route choice behavior in the upcoming era of connected vehicles. However, several limitations and some following researches should be noted for this study.

- Due to the shortage of widely used method which is able to model the relationship between road safety reliability and relevant risk factors, only the average driving speed are involved in shaping the CRC distribution of segment link. Our future efforts will consist of refining the segment CRC distribution by incorporating other risk factors, such as the environmental factors (e.g. adverse weather) and road specific factors.
- Since the lack of the empirical studies that investigate the travelers' behavioral characteristics of safe route choice, the trade-off behavior between travel safety and efficiency is hypothetically modeled to be a sample linear relationship. Further research should pay more attention on investigating such behavioral characteristics. The possible complex nonlinear relationships between perceived travel safety cost and travel time cost should be explicitly considered.

ACKNOWLEDGEMENTS

This work was jointly supported by: 1) The Joint Research Scheme of National Natural Science Foundation of China/Research Grants Council of Hong Kong (No. 71561167001 & N_HKU707/15); 2) The National Natural Science Foundation of China (Project No. 71701216); 3) National Key Research and Development Plan (No. 2018YFB1201601).

REFERENCES

Abdel-Aty, M., Kitamura, R., Jovanis, P., 1997. Using stated preference data for studying the effect of advanced traffic information on drivers' route choice. Transportation Research Part C 5, 39–50.

Abdel-Aty, M., Pemmanaboina, R., 2006. Calibrating a real-time traffic crash-prediction model using archived weather and ITS traffic data. IEEE Transactions on Intelligent Transportation Systems 7 (2), 167–174.

Aljahani, A., Rhodes A, Metcalfe A., 1999. Speed, speed limits and road traffic accidents under free flow conditions. Accident Analysis and Prevention 31, 161-168.

Bačkalić, S., Jovanović, D., Bačkalić, T., 2014. Reliability reallocation models as a support tools in traffic safety analysis. Accident Analysis Prevention 65, 47-52.

Bagloee, S., Asadi, M., 2016. Crash analysis at intersections in the CBD: a survival analysis model. Transportation Research Part A 94, 558-572.

Carrion, C., Levinson, D., 2012. Value of travel time reliability: A review of current evidence. Transportation Research Part A 46, 720-741.

Chapman, R., 1973. The concept of exposure. Accident Analysis Prevention 5, 95-110.

Chandra, S., 2014. Safety-based path finding in urban areas for older drivers and bicyclists. Transportation Research Part C 48, 143-157.

Charlton, S., Starkey, N., 2016. Risk in our midst: centrelines, perceived risk, and speed choice. Accident Analysis and Prevention, 95, 192-201.

Chen, A., Zhou, Z., Lam, W., 2011. Modeling stochastic perception error in the mean-excess traffic equilibrium model. Transportation Research Part B 45, 1619-1640.

Chen, A., Zhou, Z., 2010. The α-reliable mean-excess traffic equilibrium model with stochastic travel times. Transportation Research Part B 44, 493-513.

Chipman, M., MacGregor, C., Smiley, A., Lee, G., 1992. Time vs. distance as measures of exposure in driving surveys. Accident Analysis and Prevention 24, 679–684.

Dafermoss, S., 1982. Relaxation Algorithms for the General Asymmetric Traffic Equilibrium Problem. Transportation Science 16, 231-240.

De La Barra, T., Perez, B., Anez, J., 1993. Multidimensional path search and assignment. In 21st PTRC Summer Annual Meeting, University of Manchester, United Kingdom, 307-319.

Elliott, D., Keen, W., Miao, L., 2019. Recent advances in connected and automated vehicles. Journal of Traffic and Transportation Engineering In Press.

Elvik, R., 2002. Optimal speed limits: the limits of optimality models. Transportation Research Record, 1818, 32-38.

Elvik, R., Christensen, P., Amundsen, A., 2004. Speed and road accidents—an evaluation of the power model. Institute of Transportation Economics. TOI report, 740/2004, Oslo.

Fisk, C., Nguyen, S., 1982. Solution Algorithms for Network Equilibrium Models with Asymmetric User Costs. Transportation Science 16, 361-381.

Gabriel, S., Bernstein, D., 1997. The traffic equilibrium problem with non-additive path costs. Transportation Science 31, 337–348.

Gerla, M., Lee, E., Pau, G., Lee, U, 2014. Internet of vehicles: From intelligent grid to autonomous cars and vehicular clouds. In IEEE World Forum on Internet of Things 241–246.

Geyer, J., Raford, N., Pham, T., Ragland, D.R., 2006. Safety in Numbers. Data from Oakland, California. Transportation Research Record 1982, 150–154.

Goczyłla, K., Cielatkowski, J., 1995. Optimal routing in a transportation network. European Journal Operational Research 87, 214–222.

Han, C., Huang, H., Lee. J., Wang, J., 2018. Investigating varying effect of road-level factors on crash frequency across regions: A Bayesian hierarchical random parameter modeling approach. Analytic Methods in Accident Research 20, 81-91

Hauer, E., 1982. Traffic conflicts and exposure. Accident Analysis and Prevention 14, 359–364.

Hauer, E., 2002. Observational Before–After Studies in Road Safety. Pergamon/Elsevier Science, Inc., Tarrytown, New York.

Hong, J., Shankar, V., Venkataraman, N., 2016. A spatially autoregressive and heteroskedastic space-time pedestrian exposure modeling framework with spatial lags and endogenous network topologies. Analytic Methods in Accident Research, 10, 26-46.

Hossain, M., Abdel-Aty, M., Quddus, M.A., Muromachi, Y., Sadeek, S.N., 2019. Real-time crash prediction models: state-of-the-art, design pathways and ubiquitous requirements. Accident Analysis and Prevention 124, 66–84.

Huang, H., Abdel-Aty, M., 2010. Multilevel data and Bayesian analysis in traffic safety. Accident Analysis Prevention 42, 1556–1565.

Huang, H., Zhou, H., Wang, J., Chang, F., Ma, M., 2017. A multivariate spatial model of crash frequency by transportation modes for urban intersections. Analytic Methods in Accident Research 14, 10-21.

Jackson, W., Jucker, J., 1982. An Empirical Study of Travel Time Variability and Travel Choice Behavior. Transportation Science 16, 460-475.

Jalayer, M., Zhou, H., 2016. Evaluating the safety risk of roadside features for rural two-lane roads using reliability analysis. Accident Analysis Prevention 93, 101-113.

Jovanović, D., 2011. The application of reliability models in traffic accident frequency analysis. Safety

Science 49, 1246-1251.

Lee, C., Hellinga, B., Saccomanno, F., 2003. Real-time crash prediction model for the application to crash prevention in freeway traffic. Transportation Research Record: Journal of Transportation Research Board 1840, 67–77.

Liu, H., He, X., He, B., 2009. Method of successive weighted averages (MSWA) and self-regulated averaging schemes for solving stochastic user equilibrium problem. Networks and Spatial Economics, 9(4), 485-503.

Lo, H., Chen, A., 2000. Traffic equilibrium problem with route-specific costs: formulation and algorithms. Transportation Research Part B 34, 493-513.

Lo, H., Luo, X., Siu, B., 2006. Degradable transport network: travel time budget of travelers with heterogeneous risk aversion. Transportation Research Part B 40, 792-806.

Lo, H., Tung, Y., 2003. Network with degradable links: capacity analysis and design. Transportation Research Part B 37 (4), 345–363.

Mannering, F., Bhat, C., 2014. Analytic methods in accident research: methodological frontier and future directions. Analytic Methods in Accident Research 1, 1–22.

Markowitz, H., 1999. The early history of portfolio theory: 1600-1960. Financial Analysis Journal 55, 5–16.

Mcdonald, J., 1953. Relation between number of accidents and traffic volume at divided-highway intersections. Highway Research Board Bulletin, Issue Number: 74, Highway Research Board.

Nie, Y. Li, Q., 2013. An eco-routing model considering microscopic vehicle operating conditions. Transportation Research Part B 55, 154–170.

Nie, Y., 2011. Multi-class percentile user equilibrium with flow-dependent stochasticity. Transportation Research Part B 45, 1641-1659.

Oh, H., Mun, S., 2012. Design speed based reliability index model for roadway safety evaluation. Ksce Journal of Civil Engineering 16, 845-854.

Park, J., Abdel-Aty, M., Wu, Y., Mattei, I., 2018. Enhancing in-vehicle driving assistance information under connected vehicle environment. IEEE Transactions on Intelligent Transportation Systems 99, 1-10.

Payyanadan, R., Sanchez, F., Lee, J., 2017. Assessing Route Choice to Mitigate Older Driver Risk. IEEE Transactions on Intelligent Transportation Systems 18, 527-536.

Qin, X., Ivan, J., Ravishanker, N., 2004. Selecting exposure measures in crash rate prediction for two-lane highway segments. Accident Analysis and Prevention, 36, 183-191.

Rilett, L., Benedek, C., 1994. Traffic assignment under environmental and equity objectives. Transportation Reseach Record 1443, 92-92.

Shao, H., Meng, Q., Tam, M., 1985. Demand-driven traffic assignment problem based on travel time reliability. Transportation Research Record 2006, 220-230.

Shao H., Lam W., Mei L., 2006. A Reliability-Based Stochastic Traffic Assignment Model for Network with Multiple User Classes under Uncertainty in Demand. Networks & Spatial Economics 6, 173-204.

Smith T., Hsu C., Hsu Y., 2008. Stochastic User Equilibrium Model with Implicit Travel Time Budget Constraint. Transportation Research Record 2085, 95-103.

Tzeng, G., Chen, C., 1993. Multiobjective decision making for traffic assignment. IEEE Transactions on Engineering Management 40 (2), 180–187.

Uchida, T., Iida, Y., 1993. , Risk assignment: a new traffic assignment model considering risk of travel time variation. In: Daganzo, C. (Ed.), Proceedings of the 12th International Symposium on Transportation and Traffic Theory. Elsevier, Amsterdam, pp. 89–105.

Von, N., Morgenstern, O., 1944. Theory of Games and Economic Behavior. Princeton University Press.

Wong, S., Sze, N., Li, Y., 2007. Contributory factors to traffic crashes at signalized intersections in Hong Kong. Accident Analysis and Prevention 39, 1107-1113.

Xu, C., Wang, X., Yang, H., Xie, K., Chen, X., 2019. Exploring the impacts of speed variances on safety performance of urban elevated expressways using GPS data. Analytic Methods in Accident Research 123, 29-38.

Xie, K., Wang, X., Ozbay, K., Yang, H., 2014. Crash frequency modeling for signalized intersections in a high-density urban road network. Analytic Methods in Accident Research 2, 39-51.

Xin, P., Wong, S., Sze, N.N., 2012. The roles of exposure and speed in road safety analysis. Accident Analysis and Prevention 48, 646-471.

Xu, G., Liu, W., Yang, H., 2018. A reliability-based assignment method for railway networks with heterogeneous passengers. Transportation Research Part C 93, 501-524.

Xu, X., Chen, A., Cheng, L., Lo, H., 2014a. Modeling distribution tail in network performance assessment: a mean-excess total travel time risk measure and analytical estimation method. Transportation Research Part B 66, 32–49 .

Xu, X., Chen, A., Zhou, Z., Cheng, L., 2014b. A multi-class mean-excess traffic equilibrium model with elastic demand. Journal of Advanced Transportation 48 (3), 203–222 .

Xu, X., Wong, S., Choi, K., 2014c. A two-stage bivariate logistic-Tobit model for the safety analysis of signalized intersections. Analytic Methods in Accident Research 3-4, 1-10.

Xu, X., Chen, A., Cheng, L., Yang, C., 2017. A link-based mean-excess traffic equilibrium model under uncertainty. Transportation Research Part B 95, 53-75.

Yu, B., Chen, Y., Wang, R., Dong, Y., 2016. Safety reliability evaluation when vehicles turn right from urban major roads onto minor ones based on driver's visual perception. Accident Analysis Prevent 95, 487-494.